

2

Convective Instability

The mechanism of convective instability is intuitively straightforward: dense fluid sinks under the action of gravity, while light fluid rises to take its place. Familiar examples include water heated on a stove, cumulus clouds (Figure 2.1a), and the slow currents in the Earth's mantle that drive continental drift (Figure 2.1b). The mechanism is complicated by the action of viscosity and diffusion, which tend to oppose the instability.

In the simplest convection problems, no differential equations must be solved; the problem is entirely algebraic. In this simple context, we will introduce several important concepts that will be used repeatedly when we address more complicated problems. Watch for the following:

- normal modes,
- the fastest-growing mode,
- isomorphism,
- scaling, and
- critical states.

We will also introduce the use of the Dirac delta function in modeling instabilities.

2.1 The Perturbation Equations

We begin with the equations of motion developed in section 1.5, assuming that the Coriolis effect is negligible. We collect the equations here for convenience:

$$\vec{\nabla} \cdot \vec{u} = 0 \quad (2.1)$$

$$\frac{D\vec{u}}{Dt} = -\vec{\nabla}\pi + b\hat{e}^{(z)} + \nu\nabla^2\vec{u} \quad (2.2)$$

$$\frac{Db}{Dt} = \kappa\nabla^2 b. \quad (2.3)$$

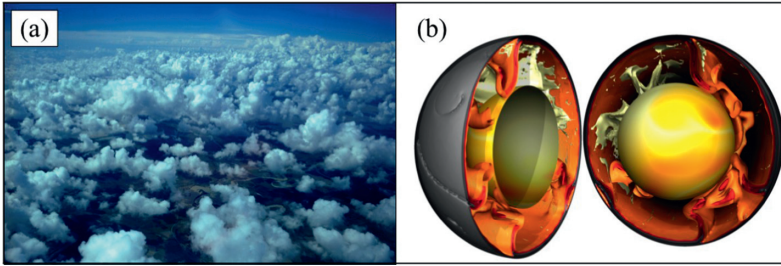


Figure 2.1 Examples of convection in geophysical flows. (a) Atmospheric convection cells revealed by cloud formation in the updrafts (NOAA). (b) Numerical simulation of convection in the Earth's mantle. **Gray-red**: cold surface plates sinking. **Yellow-white**: hot mantle plumes rising (courtesy F. Cramer, University of Oslo).

2.1.1 Hydrostatic Equilibrium

Under what conditions may a fluid be, and remain, motionless? In other words, if we assume that (1) $\vec{u} = 0$ and (2) $\partial/\partial t = 0$, can we extract a solution from the equations of motion?

The incompressibility condition (2.1) is satisfied automatically. The momentum equation (2.2) is a bit more complicated. First, when $\partial/\partial t = 0$ and $\vec{u} = 0$, the material derivative of any field vanishes:

$$\frac{D}{Dt} = \frac{\partial}{\partial t} + \vec{u} \cdot \vec{\nabla} = 0.$$

So, the left-hand side of (2.2) is zero. Also, with $\vec{u} = 0$, the viscous term is zero, leaving

$$0 = -\vec{\nabla}\pi + b\hat{e}^{(z)},$$

expressing **hydrostatic balance** between the pressure and buoyancy fields. The horizontal components give

$$\frac{\partial\pi}{\partial x} = \frac{\partial\pi}{\partial y} = 0.$$

Therefore, pressure is a function of z only. In this book we denote equilibrium fields with uppercase letters, so the hydrostatic pressure is

$$\boxed{\pi = \Pi(z)}. \quad (2.4)$$

From the vertical component we have

$$\frac{\partial\pi}{\partial z} = b,$$

or

$$b = B(z) = \frac{d\Pi}{dz} \quad (2.5)$$

Finally we have the diffusion equation for buoyancy, (2.3). As with (2.2), the material derivative on the left-hand side is zero. Using (2.5), we obtain

$$\kappa \frac{d^2 B}{dz^2} = 0. \quad (2.6)$$

We sometimes assume that κ is vanishingly small, in which case (2.6) is satisfied automatically. Otherwise, B must be a linear function of z :

$$B = B_0 + \frac{dB}{dz} z, \quad \text{where} \quad \frac{dB}{dz} \equiv B_z = \text{constant}. \quad (2.7)$$

The derivative dB/dz is the square of the **buoyancy**, or **Brunt-Väisälä**, frequency, often denoted as N^2 . What (2.7) tells us is that, for equilibrium, dB/dz must be constant; otherwise, the buoyancy profile will evolve due to diffusion. We abbreviate dB/dz as B_z .

Together with the assumption $\vec{u} = 0$, (2.4), (2.5), and (2.7) define the motionless (or “static”) equilibrium state.

2.1.2 Small Departures from Equilibrium: the Linearized Equations

Here we will derive a pair of equations that govern the evolution of small disturbances to a motionless fluid. We begin by assuming that buoyancy, pressure, and velocity are close to hydrostatic equilibrium:

$$b = B(z) + \epsilon b'(\vec{x}, t), \quad (2.8)$$

$$\pi = \Pi(z) + \epsilon \pi'(\vec{x}, t), \quad (2.9)$$

$$\vec{u} = 0 + \epsilon \vec{u}'(\vec{x}, t). \quad (2.10)$$

We refer to B and Π as the “background state” and to the primed quantities as the “perturbations.” The evolution of the perturbations is our main focus. We have introduced the ordering parameter ϵ . In perturbation theory, many quantities are assumed to be “small,” and ϵ is basically a bookkeeping trick that will help us keep track of them. Any quantity proportional to ϵ is “small”; anything proportional to ϵ^2 is “really small,” etc. (See section 1.7 for a more rigorous discussion.)

We now substitute (2.8–2.10) into the equations of motion, (2.1), (2.2), and (2.3). We start with the easiest one: $\vec{\nabla} \cdot \epsilon \vec{u}' = 0$, and therefore

$$\vec{\nabla} \cdot \vec{u}' = 0. \quad (2.11)$$

The second-simplest equation is (2.3). We work on the left-hand and right-hand sides separately. The left-hand side is:

$$\begin{aligned} \frac{Db}{Dt} &= \left(\frac{\partial}{\partial t} + \epsilon \vec{u}' \cdot \vec{\nabla} \right) (B(z) + \epsilon b') \\ &= \frac{\partial B}{\partial t} + \epsilon \vec{u}' \cdot \vec{\nabla} B(z) + \epsilon \frac{\partial b'}{\partial t} + \epsilon^2 \vec{u}' \cdot \vec{\nabla} b' \\ &= 0 + \epsilon w' \frac{dB}{dz} + \epsilon \frac{\partial b'}{\partial t} + 0 \\ &= \epsilon \left(\frac{\partial b'}{\partial t} + w' \frac{dB}{dz} \right). \end{aligned}$$

The first term, $\partial B/\partial t$, is zero by construction. The term proportional to ϵ^2 (red) is neglected because it is the product of two small quantities and is therefore “really small.”

On the right-hand side,

$$\kappa \nabla^2 b = \kappa \frac{d^2 B}{dz^2} + \epsilon \kappa \nabla^2 b'.$$

From (2.6) the first term on the right is zero. As a result, (2.3) becomes:

$$\boxed{\frac{\partial b'}{\partial t} + w' B_z = \kappa \nabla^2 b'}. \quad (2.12)$$

Recall from (2.6) that either (1) $\kappa \neq 0$ and B_z is a constant, or (2) $\kappa = 0$ and B_z is an arbitrary function of z . The second term on the left describes perturbations to the local buoyancy as a result of vertical motions advecting the “background” buoyancy (i.e., that found in the static equilibrium state).

Two important aspects of (2.12) should be noted.

- (2.12) is a *linear* equation, because the nonlinear term $\epsilon^2 \vec{u}' \cdot \vec{\nabla} b'$ has been discarded.
- The ordering parameter ϵ does not appear.

Finally we address the momentum equation (2.2). The left-hand side is

$$\frac{D\vec{u}}{Dt} = \left(\frac{\partial}{\partial t} + \epsilon \vec{u}' \cdot \vec{\nabla} \right) \epsilon \vec{u}' = \epsilon \frac{\partial \vec{u}'}{\partial t},$$

where once again the $O(\epsilon^2)$ term has been discarded. The remaining substitutions are straightforward:

$$\begin{aligned} \epsilon \frac{\partial \vec{u}'}{\partial t} &= -\vec{\nabla}(\Pi + \epsilon\pi') + (B + \epsilon b')\hat{e}^{(z)} + \nu \nabla^2 \epsilon \vec{u}' \\ &= -\frac{d\Pi}{dz}\hat{e}^{(z)} + B\hat{e}^{(z)} - \epsilon \vec{\nabla}\pi' + \epsilon b'\hat{e}^{(z)} + \epsilon \nu \nabla^2 \vec{u}'. \end{aligned} \tag{2.13}$$

From (2.5), we see that the first two terms on the right-hand side add up to zero.¹ The remaining terms are all proportional to ϵ , which therefore cancels, leaving:

$$\boxed{\frac{\partial \vec{u}'}{\partial t} = -\vec{\nabla}\pi' + b'\hat{e}^{(z)} + \nu \nabla^2 \vec{u}'}. \tag{2.14}$$

Once again, the equation is linear and does not involve ϵ . We now have a closed system: (2.11), (2.12), and (2.14) comprise five equations for the five unknowns u' , v' , w' , b' , and π' .

Note that (2.12) actually involves only two of these unknowns: w' and b' . Life could be made much easier if we could find another equation involving only those unknowns, for then we would have only two equations to solve. A good place to start is the vertical component of (2.14):

$$\frac{\partial w'}{\partial t} = -\frac{\partial \pi'}{\partial z} + b' + \nu \nabla^2 w'. \tag{2.15}$$

This involves three unknowns, but we can eliminate the pressure as follows. We begin by taking the divergence of (2.14):

$$\vec{\nabla} \cdot \frac{\partial \vec{u}'}{\partial t} = -\vec{\nabla} \cdot \vec{\nabla}\pi' + \vec{\nabla} \cdot (b'\hat{e}^{(z)}) + \vec{\nabla} \cdot \nabla^2 \vec{u}',$$

or,

$$\frac{\partial}{\partial t} \underbrace{(\vec{\nabla} \cdot \vec{u}')}_{=0} = -\nabla^2 \pi' + \frac{\partial b'}{\partial z} + \nabla^2 \underbrace{(\vec{\nabla} \cdot \vec{u}')}_{=0}.$$

The first and last terms vanish by (2.11), and we are left with a Poisson equation for π' in terms of b' :

$$\boxed{\nabla^2 \pi' = \frac{\partial b'}{\partial z}}. \tag{2.16}$$

Now take the Laplacian of (2.15):

$$\frac{\partial}{\partial t} \nabla^2 w' = -\frac{\partial}{\partial z} \nabla^2 \pi' + \nabla^2 b' + \nu \nabla^4 w',$$

¹ Another way to think about this is to recognize that, other than being $\ll 1$, ϵ can take *any* value. Therefore, the only way that (2.13) can be valid is if the terms proportional to each power of ϵ balance separately. See section 1.7.1 for a fuller discussion.

and substitute from (2.16):

$$\begin{aligned}\frac{\partial}{\partial t} \nabla^2 w' &= -\frac{\partial^2 b'}{\partial z^2} + \nabla^2 b' + \nu \nabla^4 w' \\ &= \nabla_H^2 b' + \nu \nabla^4 w',\end{aligned}$$

where

$$\nabla_H^2 = \frac{\partial^2}{\partial x^2} + \frac{\partial^2}{\partial y^2}.$$

Success! We now have two equations in two unknowns:

$$\frac{\partial}{\partial t} \nabla^2 w' = \nabla_H^2 b' + \nu \nabla^4 w', \quad (2.17)$$

$$\frac{\partial}{\partial t} b' = -B_z w' + \kappa \nabla^2 b'. \quad (2.18)$$

In the following subsections we will look at solutions of these equations in three cases of increasing complexity. We'll begin by neglecting viscosity and diffusion. We'll then restore those effects, and finally we'll add upper and lower boundaries.

2.2 Simple Case: Inviscid, Nondiffusive, Unbounded Fluid

We first investigate the highly simplified case $\nu = \kappa = 0$, in which (2.17) and (2.18) are

$$\frac{\partial}{\partial t} \nabla^2 w' = \nabla_H^2 b'; \quad \frac{\partial}{\partial t} b' = -B_z w'.$$

Applying $\partial/\partial t$ to the first of these and substituting from the second, we obtain

$$\frac{\partial^2}{\partial t^2} \nabla^2 w' = -B_z \nabla_H^2 w'. \quad (2.19)$$

For now, we will assume that B_z is a constant, but later in this subsection we will consider more general forms of B_z .

2.2.1 The Normal Mode Solution

In this simple context we will introduce a flow structure that will be used repeatedly in this course: the **plane-wave**, or **normal mode** perturbation. For the vertical velocity, this has the form

$$W(\vec{x}, t) = \hat{w} \exp\{i(kx + \ell y + mz - \omega t)\}, \quad (2.20)$$

Several aspects of (2.20) should be noted:

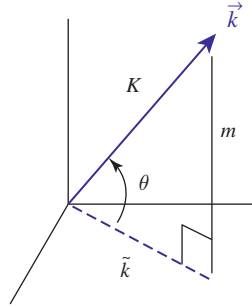


Figure 2.2 Definition sketch for the wavevector \vec{k} and its horizontal and vertical projections \tilde{k} and m .

- $\iota = \sqrt{-1}$.
- The **amplitude** \hat{w} is a complex constant.
- While W is a complex function, only the real part is physically relevant:

$$w' = W_r.$$

- $\{k, \ell, m\} = \vec{k}$ is the **wave vector** (Figure 2.2). Its components k, ℓ , and m are the **wavenumbers** corresponding to the x, y , and z directions, and are assumed to be real. The corresponding periodicity intervals (or **wavelengths**) are $2\pi/k, 2\pi/\ell$, and $2\pi/m$, respectively. In MKS units, \vec{k} is measured in m^{-1} .
- We define the **magnitude** of the wave vector $K = \sqrt{k^2 + \ell^2 + m^2}$ and its horizontal part $\tilde{k} = \sqrt{k^2 + \ell^2}$.
- The **angle of elevation**, measured from the horizontal plane, is θ , so that $\tilde{k} = K \cos \theta$ and $m = K \sin \theta$. Since $\tilde{k} \geq 0$ by definition, $-\pi/2 < \theta \leq \pi/2$.
- ω is the **complex frequency**. In MKS units, ω is measured in s^{-1} .
- The real part of ω is interpreted as the **angular frequency**, measured in radians per second. Dividing by 2π gives the **cyclic frequency** f , measured in cycles per second.
- If ω has a nonzero imaginary part, it represents exponential growth or decay.

The solution form (2.20) is more general than it may seem, because the equations (2.19 in this case) are linear and therefore obey the *principle of superposition*: two solutions can be added to make a third solution. Using the techniques of Fourier analysis, any perturbation can be expressed as a sum of expressions like (2.20).

When we substitute normal mode solutions such as (2.20) into (2.19), or (2.17), considerable simplification results as derivatives are replaced by multiplications. For example, differentiating (2.20) with respect to x produces the factor ik but otherwise changes nothing. We now list the most common differential operations and how they apply to (2.20):

$$\frac{\partial}{\partial t} \rightarrow -i\omega, \quad \text{or} \quad \frac{\partial}{\partial t} \rightarrow \sigma \quad (2.21)$$

$$\vec{\nabla} \rightarrow i\vec{k}, \quad \text{e.g.,} \quad \frac{\partial}{\partial x} \rightarrow ik \quad (2.22)$$

$$\nabla^2 \rightarrow -K^2 \quad (2.23)$$

$$\nabla_H^2 \rightarrow -\tilde{k}^2. \quad (2.24)$$

After we substitute these expressions, (2.19) becomes

$$(-\omega^2)(-K^2)W = -B_z(-\tilde{k}^2)W = 0$$

or

$$(\omega^2 K^2 - B_z \tilde{k}^2)W = 0.$$

If there is a nonzero perturbation ($w' \neq 0$), the expression in parentheses must vanish:

$$\omega^2 = B_z \frac{\tilde{k}^2}{K^2} = B_z \cos^2 \theta. \quad (2.25)$$

You may recognize this as the dispersion relation for internal gravity waves. However, the gravity wave solution applies only when $B_z > 0$.

2.2.2 Instabilities and the Fastest-Growing Mode

What if $B_z < 0$, i.e., if dense fluid overlies light fluid? In that case $\omega^2 < 0$. Writing

$$\omega = i\sigma,$$

(2.25) gives

$$\sigma = \pm \sqrt{-B_z} \cos \theta. \quad (2.26)$$

When σ is positive the mode is identified as **unstable**. Because $e^{-i\omega t} = e^{\sigma t}$, we can identify σ as an **exponential growth rate**. Like ω , σ is measured in s^{-1} .

The Fastest-Growing Mode

Naturally occurring flows are never as simple as the equilibrium state we defined in section 2.1.1; there is almost always an additional component consisting of small-scale, quasi-random fluctuations. According to Fourier's theorem, the fluctuations are equivalent to a superposition of normal modes like (2.20) with a range of ω and \vec{k} (and hence θ) connected by a dispersion relation such as (2.25) or, equivalently, (2.26).

If a given \vec{k} represents a maximum of σ , then that mode will grow the fastest. Because the growth is exponential, even a small difference in σ can make a big

difference to the amplitude later on. We usually *assume* that the initial fluctuations are infinitesimal (far too small to be detectable), so that by the time the disturbance grows to visible amplitude, this so-called **fastest-growing mode (FGM)** will dominate. Based on this assumption, we focus our attention on the FGM.

*Fastest-Growing Mode of Convection for an Inviscid,
Nondiffusive Fluid*

In the present case, (2.26) shows that the FGM has $\cos \theta = 1$, so that $\theta = 0$ and $m = K \sin \theta = 0$. The wave vector is purely horizontal. Motions associated with the fastest-growing mode are purely vertical,² which stands to reason because **vertical motions are oriented ideally to respond to gravity**.

The FGM therefore consists of spatially alternating columns of upward and downward motion, i.e., updrafts and downdrafts (Figure 2.3). The wavelength (the distance between updrafts, say) is $2\pi/\tilde{k}$. The growth rate is $\sqrt{-B_z}$. A property of particular importance in this example is that, while the growth rate depends on the orientation of the wave vector, it does not depend on its magnitude. As a result, the FGM can have any wavelength, including arbitrarily large and small wavelengths. A random noise field can grow to produce a random distribution of updrafts and downdrafts on a wide range of scales. This is called a **broadband** instability (e.g., Figure 2.4). In section 2.3 we'll re-introduce viscosity and diffusion and see how this can produce an FGM with a single, well-defined wavelength.

Classification of Normal Modes

In the case studied here (perturbations of a motionless, inviscid, nondiffusive fluid with B_z a negative constant), the growth rate has turned out to be purely real

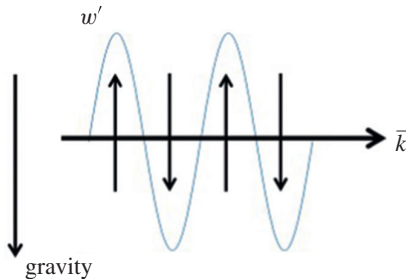


Figure 2.3 Normal mode in an inviscid, nondiffusive, uniformly stratified fluid. The wavevector is horizontal (i.e., $\theta = 0$); hence the motions are vertical. This orientation “feels” gravity most strongly: it exhibits the fastest oscillations when $B_z > 0$ (see equation 2.25), and the fastest exponential growth when $B_z < 0$ (equation 2.26).

² To verify this, note that the normal mode form of (2.16) is $-K^2 \hat{\pi} = im\hat{b}$ and, since $m = 0$ and $K^2 \neq 0$ for the FGM, there is no pressure perturbation. Examination of the horizontal components of (2.14) then shows that, with $\pi' = 0$, there is no horizontal velocity perturbation.

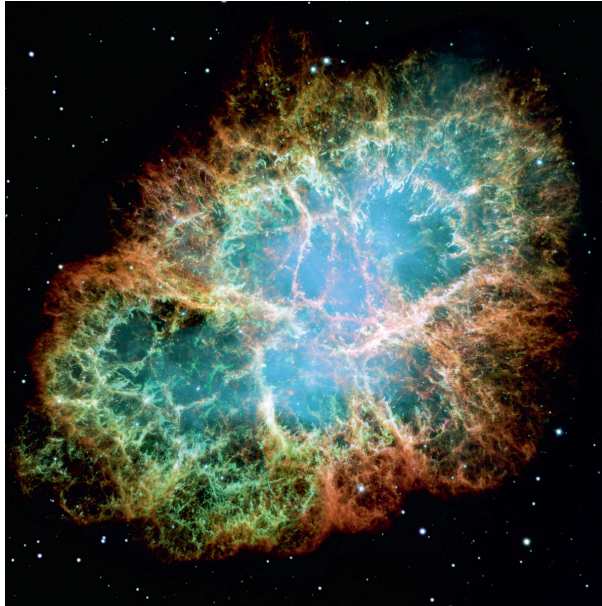


Figure 2.4 Filaments formed by Rayleigh-Taylor convective instability (section 2.2.4) in a supernova, the Crab Nebula. A rapidly expanding shell of dense ejecta is gradually decelerated as it accumulates circumstellar material, leaving it convectively unstable. Photographic mosaic created by the Hubble Space Telescope, completed January 2000, courtesy of the US National Aeronautics and Space Administration (NASA).

[recall 2.26]. We will soon see that this is true for arbitrary B_z as well. In general, though, σ also has an imaginary part, which represents an oscillatory component of the motion:

$$\sigma = \sigma_r + i\sigma_i.$$

Some terminology:

- When $\sigma_r > 0$, the solution grows exponentially and is called an unstable mode, or an **instability**. (Conversely, solutions with $\sigma_r < 0$ are called decaying modes. Those are of less interest here.)
- We define the **e-folding time** $1/\sigma_r$, the time needed for an unstable disturbance to grow by a factor of $e = 2.71828$.
- When $\sigma_i = 0$ [as is the case in (2.26) with $B_z < 0$, for example], we have **stationary** instability.
- If σ_i were *nonzero* (and $\sigma_r > 0$) the instability would be called **oscillatory**, and would have the form of an exponentially growing oscillation. We will see examples of this later.

- If $\sigma_r = 0$ and $\sigma_i \neq 0$, the solution represents a wave that propagates without change of amplitude. The internal gravity wave described by (2.26) with $B_z > 0$ is an example.
- The normal mode form (2.20) can be written in terms of σ :

$$W(\vec{x}, t) = \hat{w} e^{\sigma t + i(kx + \ell y + mz)} \tag{2.27}$$

2.2.3 Instabilities of an Arbitrary Buoyancy Profile

In the foregoing sections 2.2.1 and 2.2.2, we explored normal mode solutions for the simple case in which B_z is a constant. However, in the nondiffusive fluid that we consider in this section, any buoyancy profile $B(z)$ can remain steady. Therefore, the theory may be applied to the wide range of buoyancy profiles found in geophysical fluids if diffusion is considered negligible.

Suppose that B_z is an arbitrary function of z . Equation (2.19) is still valid, but it now has coefficients that vary with z , and therefore (2.20) is no longer a solution. Instead, we use the more general normal mode form

$$W(\vec{x}, t) = \hat{w}(z) e^{i(kx + \ell y) + \sigma t}, \tag{2.28}$$

where the complex amplitude $\hat{w}(z)$ is a function of height whose form is yet to be determined. The wave vector $\vec{k} = (k, \ell)$ is now directed entirely in the horizontal. The vertical wavenumber component, m , the three-dimensional magnitude, K , and the angle of elevation, θ , are no longer relevant. As before, only the real part is retained: $w' = W_r$.

Substituting in (2.19), we obtain

$$\sigma^2 \left(\frac{d^2}{dz^2} - \tilde{k}^2 \right) \hat{w} = B_z \tilde{k}^2 \hat{w}. \tag{2.29}$$

This is not an algebraic equation, as in sections 2.2.1 and 2.2.2, but rather is a second-order ordinary differential equation. In general, (2.29) must be solved numerically. Numerical solution methods will be discussed in the next chapter. For now, we'll derive a general theorem that tells us something important about the instability.

Suppose that the fluid is confined between two horizontal planes $z = z_1$ and $z = z_2$ where $\hat{w} = 0$. These may represent impermeable boundaries, or boundaries at infinity where the amplitude goes to zero. We now multiply (2.29) by the complex conjugate \hat{w}^* and integrate the result over the vertical domain:

$$\sigma^2 \int_{z_1}^{z_2} \left(\hat{w}^* \frac{d^2 \hat{w}}{dz^2} - \tilde{k}^2 \hat{w}^* \hat{w} \right) dz = \int_{z_1}^{z_2} B_z \tilde{k}^2 \hat{w}^* \hat{w} dz. \tag{2.30}$$

The first term in parentheses can be integrated by parts:

$$\int_{z_1}^{z_2} \hat{w}^* \frac{d^2 \hat{w}}{dz^2} dz = \hat{w}^* \frac{d\hat{w}}{dz} \Big|_{z_1}^{z_2} - \int_{z_1}^{z_2} \frac{d\hat{w}^*}{dz} \frac{d\hat{w}}{dz} dz = - \int_{z_1}^{z_2} \left| \frac{d\hat{w}}{dz} \right|^2 dz. \tag{2.31}$$

Substituting in (2.30), we have

$$\sigma^2 \int_{z_1}^{z_2} \left(- \left| \frac{d\hat{w}}{dz} \right|^2 - \tilde{k}^2 |\hat{w}|^2 \right) dz = \int_{z_1}^{z_2} B_z \tilde{k}^2 |\hat{w}|^2 dz. \tag{2.32}$$

Close inspection of (2.32) yields three useful observations.

- While σ^2 may be complex in general, in this case it is purely real [since every other quantity in (2.32) is real]. As a result, solutions separate cleanly into two categories:
 - (i) $\sigma^2 > 0$, a growing mode and a decaying mode
 - (ii) $\sigma^2 < 0$, a pair of waves propagating in opposite directions.
- Suppose that B_z is positive throughout $z_1 < z < z_2$. In that case the integral on the right-hand side of (2.32) must be positive. On the left-hand side, the quantity in parentheses is negative, and hence $\sigma^2 < 0$. The solution represents a wave, not an instability, i.e., category 1 above.
- The solution represents instability ($\sigma^2 > 0$, category 1) if the right-hand side is negative. This requires, at least, that the minimum value of B_z in $z_1 < z < z_2$ be negative. The latter is a *necessary* condition for $\sigma^2 > 0$, but it is not *sufficient*; the sufficient condition is that (1) there be some z where $B_z < 0$ and (2) the vertical motions be concentrated in that region enough to make the integral $\int_{z_1}^{z_2} B_z |\hat{w}|^2 dz$ negative.

With a bit of rearranging we can place an upper bound on the growth rate. After moving the second term to the right-hand side, (2.32) becomes

$$\sigma^2 \int_{z_1}^{z_2} \left| \frac{d\hat{w}}{dz} \right|^2 dz = - \int_{z_1}^{z_2} (\sigma^2 + B_z) \tilde{k}^2 |\hat{w}|^2 dz. \tag{2.33}$$

For $\sigma^2 > 0$, the left-hand side, and hence the right-hand side, must be positive. This means that the integrand on the right must be negative somewhere in $z_1 < z < z_2$, and therefore the *minimum* value of B_z must not only be negative (as we already know) but must also be less than $-\sigma^2$. Rearranging this inequality, we have

$$\sigma < \sqrt{-\min_z B_z}. \tag{2.34}$$

You can check this by comparing with (2.26) and with homework problems 6 and 16.

We will also find that the upper bound (2.34) is actually reached (to arbitrary precision), provided only that $B_z > 0$ for some z . In that case

$$\lim_{\tilde{k} \rightarrow \infty} \sigma = \sqrt{-\min_z B_z}. \quad (2.35)$$

You can learn more about this important result in section 7.8.1 and project B.7.

2.2.4 Convection at an Interface – Rayleigh-Taylor Instability

We now examine instabilities that arise from convection between two layers of inviscid, nondiffusive fluid with different buoyancy by solving (2.29) with the appropriate function $B(z)$. We place the interface at $z = 0$ and define buoyancy with respect to the lower layer, so that the background buoyancy profile has the step function form:

$$B(z) = \begin{cases} b_0, & z > 0 \\ 0, & z < 0 \end{cases} \quad (2.36)$$

When dealing with discontinuous profiles like (2.36), it will be helpful to use a general notation to represent the jump in a quantity, f say, occurring at the level $z = z_i$:

$$[[f]]_{z_i} \equiv f(z_i^+) - f(z_i^-). \quad (2.37)$$

Obviously $[[f]] = 0$ for a continuous function. But in (2.36), the jump in buoyancy at $z = 0$ is $[[B]]_0 = b_0$.

The buoyancy gradient, B_z , is expressed in terms of the Dirac delta function: $B_z = b_0 \delta(z)$. If the delta function is unfamiliar to you, spend some time looking at Figure 2.5.

For $z \neq 0$, $B_z = 0$ (see property 2 in Figure 2.5). Therefore, in both the upper and lower layers, (2.29) becomes

$$\frac{d^2 \hat{w}}{dz^2} - \tilde{k}^2 \hat{w} = 0. \quad (2.38)$$

This ordinary differential equation must be solved to determine $\hat{w}(z)$ in each layer. The general solution is

$$\hat{w} = \begin{cases} A_1 e^{-\tilde{k}z} + A_2 e^{\tilde{k}z}, & \text{for } z > 0 \\ A_3 e^{-\tilde{k}z} + A_4 e^{\tilde{k}z}, & \text{for } z < 0, \end{cases}$$

where A_1 , A_2 , A_3 , and A_4 are constants to be determined. We assume that the domain is vertically unbounded, and that \hat{w} is continuous and finite for all z . Those

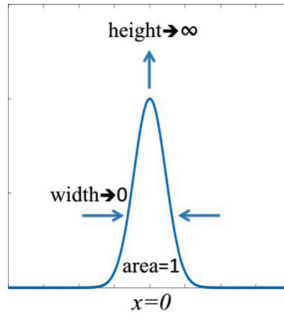


Figure 2.5 The Dirac delta function $\delta(x)$ can be thought of as a peak centered at $x = 0$, with zero width, infinite height, and unit area. It has the following properties:

1. $\delta(0) = \infty$.
2. $\delta(x) = 0$, for $x \neq 0$.
3. $\int_{-\infty}^{\infty} \delta(x) dz = 1$.
4. $\int_{-\infty}^{\infty} f(x)\delta(x) dz = f(0)$.
5. $\lim_{\epsilon \rightarrow 0} \int_{-\epsilon}^{\epsilon} f(x)\delta(x) dz = f(0)$.
6. $\lim_{\epsilon \rightarrow 0} \int_{x_0-\epsilon}^{x_0+\epsilon} f(x)\delta(x - x_0) dz = f(x_0)$.

conditions require $A_2 = 0$, $A_3 = 0$, and $A_4 = A_1$. (Show this.) Our solution can then be written compactly as

$$\hat{w}(z) = A_1 e^{-\tilde{k}|z|}. \tag{2.39}$$

Note that the largest amplitude of vertical velocity is found at the interface level, and that the motions decay with distance from the interface over a length scale proportional to the wavelength of the disturbance, \tilde{k}^{-1} .

As we have stated, \hat{w} is continuous. In fact, this is always true. (If it were not, voids would appear within the fluid, and we do not observe this.) What about its derivative? If the coefficients of our differential equation were nice, smooth functions with no infinities, \hat{w}_z would be continuous also, and this would furnish an additional constraint on the solution. But at $z = 0$, because $B_z \propto \delta(z)$, \hat{w}_z is discontinuous, as you can also see by examination of (2.39). To complete the solution, we use the properties of $\delta(z)$ to establish the change in \hat{w}_z , then require that the derivative change by that amount.

The function $\delta(x)$ has several properties (Figure 2.5) that allow us to remove it by means of integration. Here, we take advantage of property 5 by integrating (2.29) over a layer extending vertically from $z = -\epsilon$ to $z = \epsilon$, i.e.,

$$\sigma^2 \int_{-\epsilon}^{\epsilon} \left(\frac{d^2 \hat{w}}{dz^2} - \tilde{k}^2 \hat{w} \right) dz = b_0 \tilde{k}^2 \int_{-\epsilon}^{\epsilon} \delta(z) \hat{w}(z) dz, \tag{2.40}$$

and take ϵ to be vanishingly small. Integration of the first term is trivial. The second term will vanish along with ϵ , given that \hat{w} is finite. The integral on the right-hand side is simplified using property 5 of the delta function (Figure 2.5), resulting in

$$\sigma^2 \left[\left[\frac{d\hat{w}}{dz} \right] \right]_0 = b_0 \tilde{k}^2 \hat{w}(0). \quad (2.41)$$

This is called a **jump condition**, and the technique is one we'll use repeatedly in this book. For the solution (2.39),

$$\hat{w}(0) = A_1, \quad \text{and} \quad \left[\left[\frac{d\hat{w}}{dz} \right] \right]_0 = -2\tilde{k} A_1. \quad (2.42)$$

Substituting, we can solve for the growth rate:

$$\sigma = \pm \left(-\frac{b_0 \tilde{k}}{2} \right)^{1/2}. \quad (2.43)$$

Recall that for a top-heavy buoyancy profile we have $b_0 < 0$, so that instability is always present. The largest growth rates occur at the smallest scales (i.e., where \tilde{k} is large). This situation is called **ultraviolet catastrophe**. It arises here because of our neglect of viscosity and diffusion, which would damp the instability at small scales.³ We will consider these effects in the next section.

A beautiful laboratory demonstration of convective instability arising at the interface between two fluids is shown in Figure 2.6. The experimental setup consists of a rectangular container that initially separates the two fluids with a gate. In order to minimize the disturbances caused to the interface as the gate is removed, a fabric covering was used over the gate, which “peeled,” rather than “slid,” away from the interface. The removal of this gate can be seen at the left of the top panel.

If $b_0 > 0$, σ is imaginary, and the solution represents a pair of oppositely propagating gravity waves with phase speeds

$$c = \pm \left(\frac{b_0}{2\tilde{k}} \right)^{1/2}. \quad (2.44)$$

We'll encounter these waves again in Chapter 4.

2.3 Viscous and Diffusive Effects

We now return our attention to the viscous, diffusive case described by (2.17) and (2.18) with the equilibrium condition (2.7). Remember that equilibrium requires

³ In fact, due to the highly simplified setup of this problem, there are only three characteristic scales present in our problem: σ , \tilde{k} , and b_0 , and only two fundamental dimensions: length and time. This means that, before doing any stability analysis, we could have predicted from the dimensions of these parameters alone that the growth rate must scale as $\sigma \propto (b_0 \tilde{k})^{1/2}$.

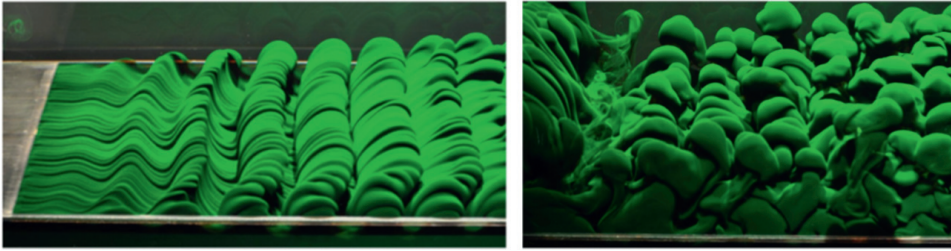


Figure 2.6 Dye visualization of convective instability at an interface (Davies Wykes, and Dalziel, 2014). Upper panel: removal of barrier (at left) 4 seconds after initial gate opening. Lower panel: 11 seconds after gate opening, disturbance is larger at the left due to peeling back of the barrier.

uniform B_z . Assuming a normal mode solution, we make the transformations (2.21–2.24) in (2.17), resulting in

$$-\sigma K^2 \hat{w} = -\tilde{k}^2 \hat{b} + \nu(-K^2)^2 \hat{w},$$

or

$$\sigma \hat{w} = \cos^2 \theta \hat{b} - \nu K^2 \hat{w},$$

and in (2.18):

$$\sigma \hat{b} = -B_z \hat{w} - \kappa K^2 \hat{b}.$$

These can be written as a 2×2 matrix eigenvalue equation, with eigenvalue σ and eigenvector $[\hat{w} \ \hat{b}]^T$:

$$\sigma \begin{bmatrix} \hat{w} \\ \hat{b} \end{bmatrix} = \begin{bmatrix} -\nu K^2 & \cos^2 \theta \\ -B_z & -\kappa K^2 \end{bmatrix} \begin{bmatrix} \hat{w} \\ \hat{b} \end{bmatrix}. \quad (2.45)$$

The eigenvalues are determined by the characteristic equation:

$$\begin{vmatrix} -\nu K^2 - \sigma & \cos^2 \theta \\ -B_z & -\kappa K^2 - \sigma \end{vmatrix} = 0,$$

or

$$\sigma^2 + (\nu + \kappa)K^2 \sigma + \nu\kappa K^4 + B_z \cos^2 \theta = 0. \quad (2.46)$$

Note that, in the limit $K^2 \rightarrow 0$, we recover the inviscid, nondiffusive result (2.25). This tells us that *viscosity and diffusivity have negligible influence on disturbances with sufficiently large spatial scale*, a common result in fluid mechanics.

In general, the solutions are

$$\sigma = \frac{1}{2} \left[-(\nu + \kappa)K^2 \pm \sqrt{\mathcal{D}} \right], \quad (2.47)$$

where the discriminant is

$$D = (\nu + \kappa)^2 K^4 - 4(\nu\kappa K^4 + B_z \cos^2 \theta).$$

There are three classes of solutions based on D :

- If $D < 0$, both values of σ are complex. Their real parts are the same:

$$\sigma_r = -\frac{(\nu + \kappa)K^2}{2},$$

and both are negative, so the flow is **stable**. The imaginary parts have opposite signs and thus represent waves propagating in opposite directions, decaying as they go.

- If $0 < D < (\nu + \kappa)^2 K^4$, then both solutions are real and negative, so the disturbance simply decays in place and the flow is classified as **stable**.
- If $D > (\nu + \kappa)^2 K^4$, both solutions are real and one has $\sigma_r > 0$, i.e., the flow is **unstable**.

The condition for instability $D > (\nu + \kappa)^2 K^4$ is equivalent to

$$\nu\kappa K^4 + B_z \cos^2 \theta < 0,$$

which can only happen if $B_z < 0$. Solving for K^2 gives

$$K^2 < \sqrt{\frac{-B_z \cos^2 \theta}{\nu\kappa}}.$$

This condition is illustrated in Figure 2.7. Differentiating (2.46) with respect to K^2 , one gets

$$2\sigma \frac{\partial \sigma}{\partial K^2} + (\nu + \kappa)K^2 \frac{\partial \sigma}{\partial K^2} + (\nu + \kappa)\sigma + 2\nu\kappa K^2 = 0,$$

or

$$\frac{\partial \sigma}{\partial K^2} = -\frac{(\nu + \kappa)\sigma + 2\nu\kappa K^2}{2\sigma + (\nu + \kappa)K^2} < 0,$$

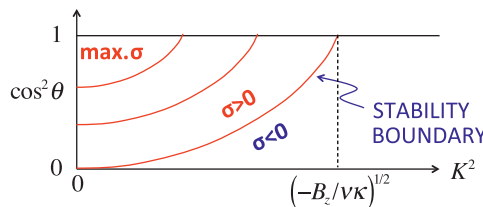


Figure 2.7 Growth rate for convection in an unbounded fluid.

which is negative in the unstable regime because σ is real and positive. In the same way, you can show that

$$\frac{\partial \sigma}{\partial \cos^2 \theta} > 0.$$

Note that

- Short waves are stabilized by viscosity and diffusion, and the effect increases as K^2 increases.
- The fastest-growing instability is found in the limit $K^2 \rightarrow 0$ and has purely vertical motions ($\cos^2 \theta = 1$) just as in the inviscid, nondiffusive case.
- In the special case $B_z = 0$ (either the fluid is homogeneous or gravity is negligible), (2.46) has two decaying solutions: $\sigma = -\nu K^2$ and $\sigma = -\kappa K^2$. Again, the smallest scales decay the fastest.
- If $B_z < 0$, the flow is unstable, i.e., there will always be some values of K and θ such that the growth rate is positive.

The fact that growth rate increases monotonically with wavelength tells us that convective instability prefers the largest possible scale, and therefore that boundary conditions are important. We'll address that issue in the next section.

2.4 Boundary Effects: the Rayleigh-Benard Problem

Consider a layer of fluid in motionless equilibrium bounded by frictionless, horizontal plates at $z = 0$ and $z = H$ (Figure 2.8). At these boundaries, w' must vanish. To satisfy that condition, we use a variant of the normal mode solution (2.20):

$$W(\vec{x}, t) = \hat{w} \sin(mz) \exp\{i(kx + \ell y) + \sigma t\}, \quad \text{where } m = n \frac{\pi}{H}; \quad n = 1, 2, \dots \tag{2.48}$$

where once again $w' = W_r$. We assume in addition that the buoyancy at the boundaries is fixed, so that $b' = 0$ and the normal mode form for buoyancy is therefore the same as (2.48). These modes have a form very different from the planar motions described by (2.20). Counter-rotating cells are arranged so that there is no vertical motion at the boundaries (Figure 2.9). The vertical scale decreases with increasing mode number n .

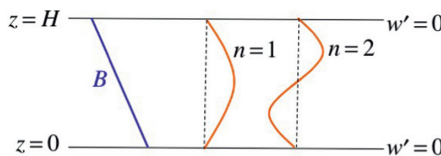


Figure 2.8 Definition sketch for Rayleigh-Benard convection.

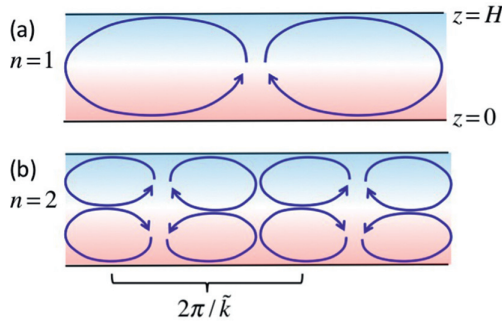


Figure 2.9 Normal modes (2.48) for the Rayleigh-Benard convection problem.

Substituting (2.48) in (2.17) and (2.18), we once again obtain (2.45); the only difference is the quantization condition $m = n\pi/H$. The characteristic equation is again (2.46), but we will now find it more convenient to write it in terms of \tilde{k} rather than $\cos \theta$:

$$\sigma^2 + (\nu + \kappa)K^2 \sigma + \nu\kappa K^4 + B_z \frac{\tilde{k}^2}{K^2} = 0. \tag{2.49}$$

Because of the quantization of m , the squared magnitude of the wave vector is now:

$$K^2 = k^2 + \ell^2 + m^2 = \tilde{k}^2 + \frac{n^2\pi^2}{H^2}; \quad n = 1, 2, \dots \tag{2.50}$$

2.4.1 Diffusion Scaling

Note that the solution of (2.49, 2.50) depends on six parameters:

$$\sigma = \mathcal{F}(\tilde{k}, n; B_z, \nu, \kappa, H). \tag{2.51}$$

The semicolon separates parameters describing the disturbance from those describing the environment it evolves in. Even though the solution for σ is relatively simple, the exploration of its properties in a six-dimensional parameter space is inefficient. We can reduce the dimensionality of the parameter space by means of *scaling*, a concept that we will use repeatedly. To set the stage for scaling, we define the concept of **isomorphism**.

Isomorphism

Two mathematical problems are **isomorphic** if they have, literally, the same form. For example, these two quadratic equations are isomorphic:

$$Ax^2 + Bx + C = 0 \tag{2.52}$$

$$\alpha y^2 + \beta y + \gamma = 0. \quad (2.53)$$

We write this relationship as (2.52) \leftrightarrow (2.53).

Now suppose we have a **solution algorithm** for (2.52). This could be an analytical formula or a subroutine. In the present example, our solution algorithm could be the quadratic formula, as implemented in the following Matlab subroutine:

```
function x = quad(A,B,C)
D = B^2-4*A*C;
x(1) = -B/2+sqrt(D)/2;
x(2) = -B/2-sqrt(D)/2;
return
```

We can use the *same* subroutine to solve (2.53); we simply substitute the appropriate variables:

```
y=quad( $\alpha$ ,  $\beta$ ,  $\gamma$ ).
```

To sum up, if two problems are isomorphic, we can solve them using the same solution algorithm with different variables.⁴ In this case we would write:

$$\begin{aligned} A &\rightarrow \alpha \\ B &\rightarrow \beta \\ C &\rightarrow \gamma \\ x &\rightarrow y. \end{aligned}$$

To apply this idea to (2.51), we define a length scale and a time scale, which we choose to be H and H^2/κ , respectively. We then use these scales to define the nondimensional variables σ^* , \tilde{k}^* , and K^* :

$$\sigma = \sigma^* \frac{\kappa}{H^2} \quad (2.54)$$

$$\tilde{k} = \frac{\tilde{k}^*}{H} \quad (2.55)$$

$$K = \frac{K^*}{H}. \quad (2.56)$$

Substituting these into (2.49), we have

$$\sigma^{*2} \frac{\kappa^2}{H^4} + (\nu + \kappa) \frac{K^{*2}}{H^2} \sigma^* \frac{\kappa}{H^2} + \nu \kappa \frac{K^{*4}}{H^4} + B_z \frac{\tilde{k}^{*2}/H^2}{K^{*2}/H^2} = 0.$$

Is this isomorphic to (2.49)? We can make the first term look the same by multiplying through by H^4/κ^2 :

⁴ Mathematicians have a more exacting definition of “isomorphism.” Here, the essential characteristic defining isomorphic equations is that a single algorithm solves both.

$$\sigma^{*2} + \left(\frac{\nu}{\kappa} + 1\right)K^{*2} \sigma^* + \frac{\nu}{\kappa}K^{*4} + \frac{B_z H^4}{\kappa^2} \frac{\tilde{k}^{*2}}{K^{*2}} = 0. \quad (2.57)$$

This form of the equation contains two new parameters: the **Prandtl number**

$$Pr = \frac{\nu}{\kappa},$$

and the **Rayleigh number**,

$$Ra = \frac{-B_z H^4}{\nu \kappa}.$$

The Prandtl number depends only on the chemical makeup of the fluid. For air, $Pr \approx 1$. For water, $Pr \approx 7$ when the stratification is thermal, 700 when the stratification is saline. The Rayleigh number quantifies the relative importance of gravity and viscosity/diffusion.⁵

Substituting the definitions of Pr and Ra in (2.57), we have

$$\sigma^{*2} + (Pr + 1)K^{*2} \sigma^* + Pr K^{*4} - Ra Pr \frac{\tilde{k}^{*2}}{K^{*2}} = 0. \quad (2.58)$$

We can also write a nondimensional version of the quantization condition (2.50):

$$K^{*2} = \tilde{k}^{*2} + n^2 \pi^2. \quad (2.59)$$

Note that (2.58) and (2.59) are isomorphic to (2.49) and (2.50). Now suppose that, in (2.51), \mathcal{F} stands for some solution algorithm for (2.49, 2.50). The same solution algorithm will then work for (2.58, 2.59), after we make the appropriate substitutions:

$$\begin{aligned} \sigma &\rightarrow \sigma^* \\ \nu &\rightarrow Pr \\ K &\rightarrow K^* \\ \kappa &\rightarrow 1 \\ B_z &\rightarrow -Ra Pr \\ \tilde{k} &\rightarrow \tilde{k}^* \\ H &\rightarrow 1, \end{aligned}$$

resulting in

$$\sigma^* = \mathcal{F}(\tilde{k}^*, n; -Ra Pr, Pr, 1, 1). \quad (2.60)$$

⁵ To see this, recall that the maximum growth rate due to gravity alone (in the absence of viscosity and diffusion; see 2.26) is $\sqrt{-B_z}$. A disturbance with length H is damped by viscosity at a rate $\sim \nu/H^2$, and by diffusion at a rate $\sim \kappa/H^2$. The Rayleigh number is therefore a nondimensional combination of rates: the gravitational growth rate (squared) divided by the product of viscous and diffusive decay rates.

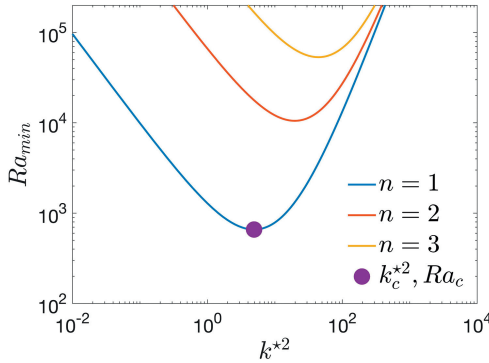


Figure 2.10 Minimum Rayleigh number for instability versus squared scaled wavenumber \tilde{k}^{*2} . The bullet shows the critical point $\tilde{k}^{*2} = \pi^2/2, Ra_c = 657.5$.

The number of independent parameters is now reduced to four, \tilde{k}^* , n , Ra , and Pr , greatly simplifying the subsequent analysis.

In this book, we will explore both numerical and analytical solutions to many instability problems. When developing subroutines, we will use dimensional variables, as in (2.51). But when exploring solutions in multidimensional parameter spaces, we will simplify the task by calling the subroutines using appropriately scaled variables, as in (2.60).

2.4.2 The Critical State for the Onset of Convective Instability

The solution of (2.58) is

$$\sigma^* = \frac{1}{2} \left[-(Pr + 1)K^{*2} \pm \sqrt{\mathcal{D}} \right],$$

where

$$\mathcal{D} = (Pr + 1)^2 K^{*4} - 4Pr \left(K^{*4} - Ra \frac{\tilde{k}^{*2}}{K^{*2}} \right).$$

This is just (2.47) with the diffusion scaling applied, but because of the boundaries we must also impose the quantization condition (2.59).

The solution is unstable if and only if

$$\mathcal{D} > (Pr + 1)^2 K^{*4},$$

or

$$K^{*4} - Ra \frac{\tilde{k}^{*2}}{K^{*2}} < 0,$$

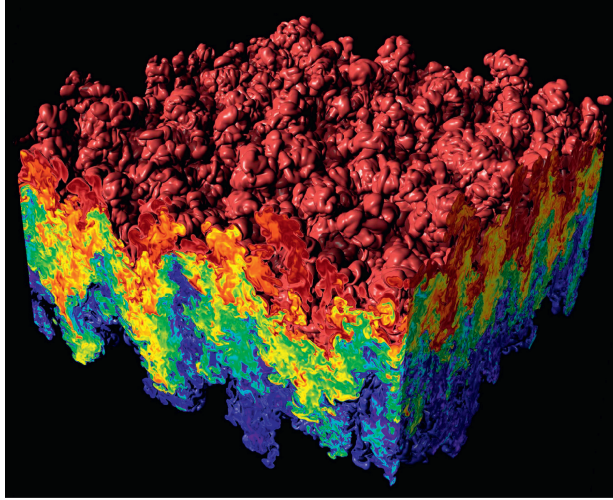


Figure 2.11 Turbulent convection in a numerical simulation. Blue (red) indicates buoyant (dense) fluid. From Cabot and Cook (2006).

or

$$Ra > \frac{(\tilde{k}^{*2} + n^2\pi^2)^3}{\tilde{k}^{*2}} \quad (2.61)$$

(see Figure 2.11).

This illustrates something interesting about the physics of convection in a bounded fluid: *it is not enough that dense fluid overlie light fluid*, i.e., $B_z < 0$, or $Ra > 0$, because disturbances amplified by gravity are simultaneously damped by viscosity and diffusion. As we saw previously in the unbounded cases (section 2.3), the relative strength of gravity and viscosity/diffusion is determined by two factors: the spatial scale of the normal mode, and the orientation of the motions. Specifically:

- Large-scale motions are relatively immune to damping by viscosity and diffusion. In the absence of boundaries, as long as $B_z < 0$, there will always be a normal mode large enough that viscosity and diffusion are too weak to prevent its growth. Boundaries limit the spatial scale, however, so that a sufficiently large wavelength may not fit.
- Gravity works most effectively on motions that are purely vertical (section 2.2.2). For a fixed value of m , as \tilde{k} decreases (i.e., for wider convection cells, see Figure 2.9), the motion becomes mainly horizontal, so the gravitational acceleration is weaker.

Because of this competition, there is an *optimal horizontal scale for growth*: a scale at which viscosity and diffusion are small but gravity is still effective. There is also

a minimum value of Ra below which even the mode with the optimum horizontal scale will not grow.

We now quantify these intuitive ideas by analyzing (2.61). Differentiating the right-hand side with respect to \tilde{k}^2 and setting the result to zero, we find that the minimum Ra for instability is smallest, for a given n , when

$$\tilde{k}^* = n\pi/\sqrt{2}.$$

With \tilde{k}^* set to this optimal value, the minimum Ra for instability is $27/4 \times n^4 \pi^4$. The higher the vertical mode number n , the higher Ra has to be (because higher n means stronger damping by viscosity/diffusion). The minimum Ra is therefore lowest when $n = 1$. The critical Ra for instability is therefore

$$Ra_c = \frac{27}{4} \pi^4 \approx 657.5.$$

The horizontal wavelength $2\pi/\tilde{k}$ is $2\sqrt{2}H$. Since a wavelength comprises two convection cells, each cell has width about 1.4 times the thickness of the convecting layer.

So, suppose that B_z starts out at zero but gradually becomes more negative, as happens when fluid is heated from below. When B_z becomes negative enough that Ra exceeds 657.5, convective motions begin. These have vertical mode number $n = 1$ (i.e., a single row of convection cells that occupy the entire vertical domain) and $\tilde{k}^* = \pi/\sqrt{2}$. Therefore, the spacing between updrafts (or between downdrafts) is about three times the layer thickness.⁶

Note that the parameters of this critical state do not depend on the Prandtl number. As a result, they apply equally well to air, seawater, magma, or any other convecting fluid.

2.5 Nonlinear Effects

While the growth rate depends on the magnitude of the horizontal wavenumber \tilde{k} , the *direction* of the wave vector (in the horizontal) is of no consequence. Therefore, a random initial perturbation will produce convection rolls with all possible horizontal orientations. By Fourier's theorem, these can sum to make a variety of planforms. Nonlinear analyses predict that the dominant planform is hexagonal (Schluter et al., 1965), and laboratory experiments have confirmed this (e.g., Figure 2.12a, also Figure 9.1). In a much more energetic environment such as the Sun's surface (Figure 2.12b), the planform is less regular.

⁶ The foregoing solution applies to a fluid with frictionless boundaries. If one assumes frictional boundaries, at which the horizontal velocity must vanish, the critical state has $Ra = 1708$.

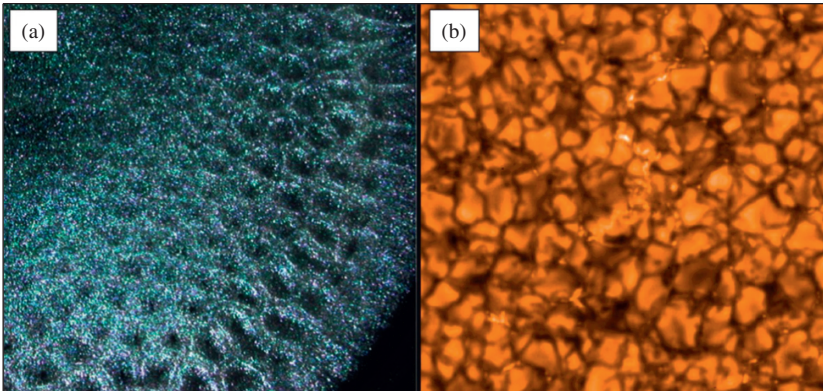


Figure 2.12 (a) Convection cells at centimeter scale in a lab experiment. A mixture of silicone oil and fine aluminum powder is heated from below. Cells form with fluid rising in the center and sinking at the edges (NOAA). (b) Convection cells at 1000 km scale in the solar photosphere. Bright (dark) regions are rising (sinking). (NASA Hinode Solar Optical Telescope, Hinode JAXA/NASA/PPARC).

In most geophysical examples of convection, Ra is many orders of magnitude greater than the critical value. Convection is turbulent, with chaotic motions over a broad range of scales (e.g., Figures 2.1 and 2.11). The vertical motion is dominated by thin plumes. The spacing of the strongest plumes is generally of the same order of magnitude as the thickness of the convecting layer, reflecting the underlying linear instability.

Linden (2000) gives a clear and detailed description of environmental convection, including the nonlinear regime.

2.6 Summary

The main “rules of thumb” about convection that one should take away from this chapter are:

- In a layer with frictionless boundaries, convection requires that $Ra > 657.5$.
- The exact value of Ra that must be exceeded for convection depends on the boundary conditions, so a more general rule of thumb is $Ra \gtrsim 10^3$.
- The spacing between updrafts (or between downdrafts) is about three times the layer thickness.

2.7 Appendix: Waves and Convection in a Compressible Fluid

Compressibility is a property of all fluids, though it is more important in some fluids (e.g., the atmosphere) and less so in others (e.g., lakes and rivers).

Compressibility mainly affects the meaning and measurement of the buoyancy gradient B_z , which is of course critical to the prediction of gravity waves and convective instability. Here we will examine the stability characteristics of a compressible fluid using the **parcel method**, a less-precise, but often more-intuitive alternative to the normal mode method. After introducing the parcel method in an incompressible fluid, we'll conduct a thought experiment aimed at understanding convection and waves in a compressible fluid. To highlight compressibility effects, we will neglect viscosity and diffusion.

2.7.1 Thought Experiment: Assessing Stability via the Parcel Method

Consider a layer of inviscid, incompressible fluid that is stably stratified, so that its vertical density gradient ρ_z is negative as shown in Figure 2.13a. Now imagine that a parcel of fluid is lifted up a distance η above its equilibrium height. If the parcel is sufficiently small, the resulting pressure change is negligible and the parcel's motion is governed only by the buoyancy force. If the displacement is rapid, there will be no exchange of heat with the surrounding fluid, and therefore no change in the density of the parcel. This is called an **adiabatic** displacement.

At its new elevation, the parcel is denser than the surrounding fluid and is therefore accelerated downward (upper **blue** arrow in Figure 2.13a). Conversely, a parcel displaced below its equilibrium height will be accelerated upward. Buoyancy therefore creates a restoring force that can support oscillatory motion.

Let's make this observation a bit more quantitative. If the vertical displacement is small, then the buoyant acceleration is $-g\Delta\rho/\rho$, where $\Delta\rho$ is the density of the parcel minus that of the surrounding fluid. To first order in η , we can approximate $\Delta\rho$ as $-\rho_z\eta$ (show this), and therefore

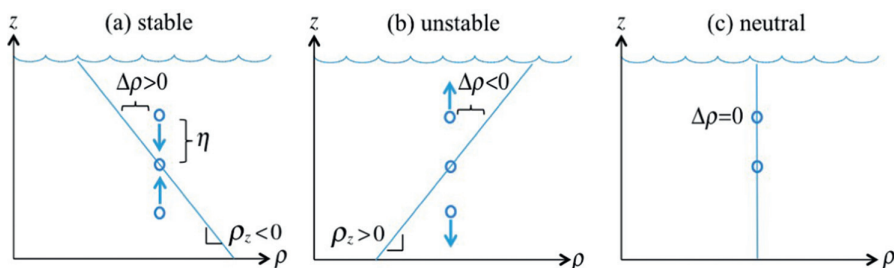


Figure 2.13 The parcel method applied to gravity waves (a), convection (b), and neutral stability (c). Circles represent small fluid parcels displaced vertically from their equilibrium heights. The density differential $\Delta\rho$ is the parcel's density minus that of the surrounding fluid. The fluid is assumed to be incompressible and the motion adiabatic, so the parcel's density remains constant as it moves.

$$\frac{d^2\eta}{dt^2} = \frac{g}{\rho}\rho_z\eta. \quad (2.62)$$

With $\rho_z < 0$, the solution is $\eta \sim e^{\pm i\omega t}$, with

$$\omega = \sqrt{-\frac{g}{\rho}\rho_z} = \sqrt{B_z}. \quad (2.63)$$

You will recognize this as the *buoyancy frequency* discussed previously in section 2.1.1. It corresponds to the frequency of an internal gravity wave, in uniform stratification, in which the motion is purely vertical, i.e., $\theta = 0$ in (2.25).

Now, what happens if the density gradient is reversed, so that $\rho_z > 0$ (Figure 2.13b)? Displaced above its equilibrium height, our fluid parcel finds itself *lighter* than its surroundings and therefore continues to rise. Conversely, a parcel displaced downward continues to sink. This is the parcel version of convective instability. The solution of (2.62) is now $\eta \sim e^{\sigma t}$, with the growth rate σ given by

$$\sigma = \sqrt{\frac{g}{\rho}\rho_z} = \sqrt{-B_z},$$

exactly as found in section 2.2 using normal modes (cf. 2.26 with $\theta = 0$).

Finally, suppose that the fluid is homogeneous (Figure 2.13c). In that case the displaced parcel has the same density as its surroundings, and it therefore feels no buoyancy force. This is the state of *neutral* stratification.

2.7.2 Another Thought Experiment: Effects of Compressibility

We'll now repeat the thought experiment described above, but our working fluid will be an imaginary substance whose compressibility we can alter at will. Consider a layer of inviscid, incompressible fluid. Beginning with the simplest case, we assume that the density is *uniform*, as in Figure 2.13c or 2.14a. Now we flip a magic switch and the fluid becomes compressible (Figure 2.14a). Picture what happens next: the surface descends slightly as the fluid is compressed under its own weight. Compression is greatest at the bottom, where the pressure is greatest. In fact, the density increase is nearly proportional to the pressure, so after compression the density gradient ρ_z will equal $-\gamma$, where γ is a constant that quantifies the degree of compressibility.⁷

Based on this negative density gradient, you might think that the fluid is now stably stratified, but you'd be wrong. Suppose that a fluid parcel is displaced upward, as in Figure 2.14a. In contrast to the incompressible case, the parcel does *not* retain

⁷ The density profile will actually be exponential, but linearity is a fine approximation for small changes.

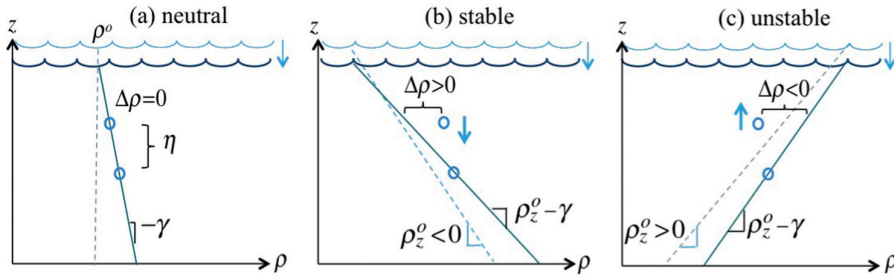


Figure 2.14 Density profiles in a fluid with (solid) and without (dashed) compression effects. Circles illustrate the change in density as a fluid parcel is raised above its equilibrium position.

its original density, but rather expands as the ambient pressure decreases. Its density decreases at exactly the same rate as that of the surrounding fluid, namely $-\gamma$, and it therefore feels *no buoyancy force*. The fluid is neutrally stable, just as when it was incompressible. Put another way, the state of neutral stability in a compressible fluid is defined not by $\rho_z = 0$ but by $\rho_z = -\gamma$.

Next, suppose that our original fluid layer is already stably stratified, with density gradient $\rho_z^o < 0$. When the fluid is allowed to compress (Figure 2.14b), its density will once again increase in proportion to pressure. The density gradient now decreases from its original, negative value ρ_z^o to the *more* negative value $\rho_z^o - \gamma$.

At a glance it looks like the fluid has become even more stable, but what happens to a lifted fluid parcel? Again, the parcel expands as the pressure is released, so that its density decreases with height at the rate $-\gamma$. The difference between the density of the parcel and its surroundings is $-\rho_z^o \eta$, and the parcel oscillates with frequency $\omega = \sqrt{-(g/\rho)\rho_z^o}$. This is superficially similar to the incompressible result (2.63), the difference being that ρ^o represents the *original* density profile, before the fluid was allowed to compress.

As a final example, suppose that the original stratification is unstable, i.e., $\rho_z^o > 0$, so that a displaced parcel will accelerate away from its equilibrium height (Figure 2.14c). The result of compression is to reduce the density gradient by adding $-\gamma$. However, the compressibility of the parcel compensates for that change, so that the displacement grows exponentially with rate $\sigma = \sqrt{(g/\rho)\rho_z^o}$.

Now here is a critical point: *the density gradient we actually observe in a compressible fluid includes the compressive part, $-\gamma$* . The original, “uncompressed” state described in our thought experiment is actually a nonexistent fiction, albeit an important one because it determines the stability of the fluid. To assess the stability of a compressible fluid like the atmosphere, we first measure the net density gradient, $\rho_z^o - \gamma$, then remove the compressive part to recover ρ_z^o . Another way to say

this is that the squared buoyancy frequency (or buoyancy gradient) B_z is given by the *observed* density gradient, ρ_z , minus the compressive part, which works out to

$$B_z = -\frac{g}{\rho}(\rho_z + \gamma). \quad (2.64)$$

So in summary, a compressible fluid is less stable (or more unstable) than it looks. The difference is the compressibility parameter γ .

2.7.3 A Quantitative View

We can quantify γ as follows:

$$\gamma = -\frac{d\rho}{dz} = -\frac{\partial\rho}{\partial p} \frac{\partial p}{\partial z}.$$

For adiabatic displacements, the partial derivative $\partial\rho/\partial p$ is the positive quantity $1/c_s^2$. We won't prove it here, but c_s turns out to be the speed of sound in the fluid. Moreover, since the ambient fluid is in equilibrium, its pressure is hydrostatic: $\partial p/\partial z = -\rho g$. Combining these results, we have

$$\gamma = \frac{\rho g}{c_s^2}. \quad (2.65)$$

In the incompressible limit, the sound speed goes to infinity, and hence $\gamma \rightarrow 0$ and $N^2 \rightarrow B_z$ (cf. 2.64) as we have found before.

In meteorology, stability is usually discussed in terms of temperature rather than density. Those who have studied such things will recognize that γ is related to the **adiabatic lapse rate** of temperature, commonly called Γ , via $\gamma = \alpha\rho\Gamma$, α being the thermal expansion coefficient. The Earth's troposphere is often found near a state of neutral stability: its temperature decreases with height at the adiabatic lapse rate, in that case typically $10^\circ\text{C}/\text{km}$.

The density in our imaginary "uncompressed" state, $\rho^o(z)$, is called **potential density**. Potential density is defined as the density a fluid parcel would have if moved adiabatically to some reference height. In our thought experiment, the reference height is the surface of the fluid layer. For a simple example, refer to Figure 2.14a. There, the uncompressed density profile (dashed line) is just a constant. In the compressed state, lifting a parcel adiabatically from any height moves it along the solid line to the surface, where its density becomes that same constant value ρ^0 .